The multi-scale environment of RS Cnc from CO and HI observations*

D. T. Hoai[1,2] , L. D. Matthews[3] , J. M. Winters[4] , P. T. Nhung[1,2] , E. Gérard[5] , Y. Libert[1,4] , and T. Le Bertre[1]

[1]LERMA, Observatoire de Paris, France; [2]VATLY/INST, Vietnam; [3]MIT Haystack Observatory, USA; [4]IRAM, France; [5]GEPI, Observatoire de Paris, France.

* *Based on observations carried out with the IRAM Plateau de Bure Interferometer and the IRAM 30m Telescope. IRAM is supported by INSU/CNRS (France), MPG (Germany) and IGN (Spain)*

We present a detailed study of the circumstellar gas distribution and kinematics of the semi-regular variable star RS Cnc on spatial scales ranging from ~1" (~150 AU) to ~6' (~0.25 pc). The close environment of RS Cnc (from 1 to 20") can be described with a model in which the density and the velocity vary smoothly from the equatorial plane to the polar axis. In this model the mass loss rate is higher along the polar directions than in the equatorial plane, which does not favor current models invoking stellar rotation or magnetic field as a cause of the axi-symmetry. Outside this region, the study of which is limited by the photo-dissociation of CO, HI data at 21 cm show that the flow is slowed down at a typical distance of 1' (~ 0.04 pc). Further away the flow is distorted by the relative motion of the star with respect to the interstellar medium (1 to 6', or 0.05 to 0.25 pc).

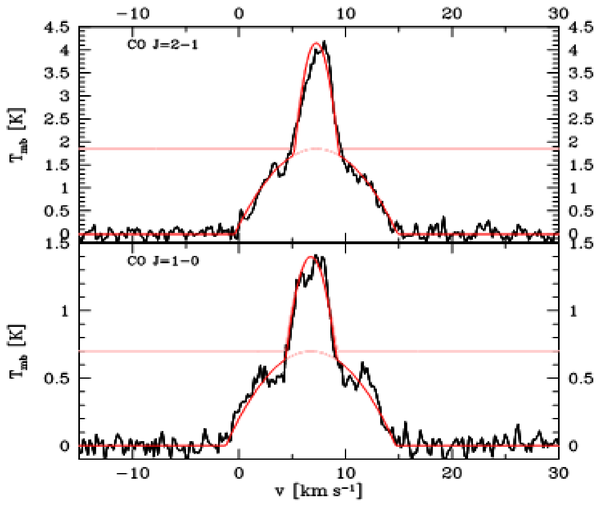

Figure 1: CO2-1 (upper) and CO1-0 (lower) spectra obtained from 30m IRAM telescope (black) and two wind model fit (red) (Libert et al. 2010).

Table 1. Properties of RS Cnc.

Parameter	Value	Ref.
Distance	143 pc	1
MK Spectral type	M6eIb-II(S)	2
Variability type	SRc:	2
Pulsation periods	122 and 248 days	3
Effective temperature	3226 K	4
Radius	225 $R_\odot$	4
Luminosity	4945 $L_\odot$	4
LSR radial velocity ($V_\star$)	6.75 km s^{-1}	5
Expansion velocity	2.4/8.0 km s^{-1}	5
Mass loss rate	1.7×10^{-7} $M_\odot$ yr^{-1}	6
3D space velocity; PA	15 km s^{-1}; 155°	this work

References. (1) Hipparcos (van Leeuwen 2007); (2) GCVS (General Catalogue of Variable Stars); (3) Adelman & Dennis (2005); (4) Dumm & Schild (1998); (5) Libert et al. (2010); (6) Knapp et al. (1998).

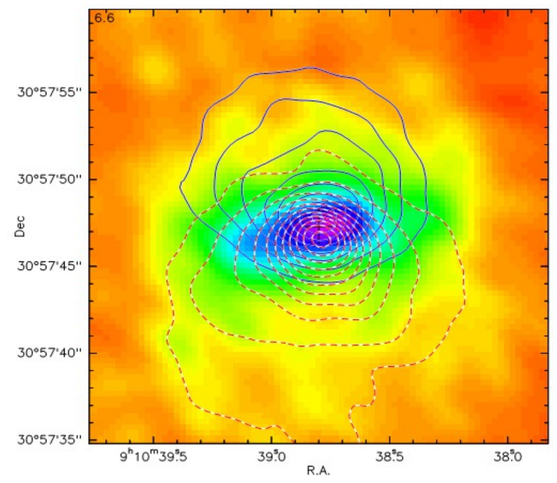

Figure 2: Bipolar structure in CO(1–0). Blue lines: emission integrated over −2 kms^{-1} to 3 kms^{-1} . Red dotted lines:emission integrated over 9.5 kms^{-1} to 16 kms^{-1} . The background image shows the 6.6 kms^{-1} channel.

CO observations

Earlier spectroscopic and interferometric observations (Knapp et al. 1998, Libert et al. 2010) show clearly the presence of two wind components which originate from two different regions: a slowly expanding (∼2 kms^{-1}) equatorial disk/waist and a faster (∼8 kms^{-1}) bipolar outflow (**Fig. 1** and **2**).

In 2011, we obtained new data of the CO1-0 line with the IRAM-PdBI array having ~2 times higher resolution. In the continuum at 115 GHz, RS Cnc is clearly detected. The source is unresolved, and there is no evidence of a companion (**Fig. 3**). However, on the line, at channel map of 6.6 kms^{-1}, we observe a possible companion at ∼1" west-northwest (PA ∼300°) (**Fig. 4**). This source is detected from 5.8 kms^{-1} to 6.8 kms^{-1}, but not outside this range. This secondary source is clearly not at the origin of the bipolar outflow, which seems to be centered on the continuum source.

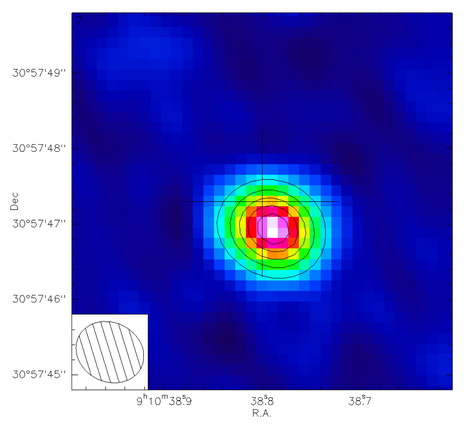

Figure 3: Continuum map at 115 GHz of RS Cnc. The contour levels are separated by steps of 0.90mJy/beam (≡20σ)

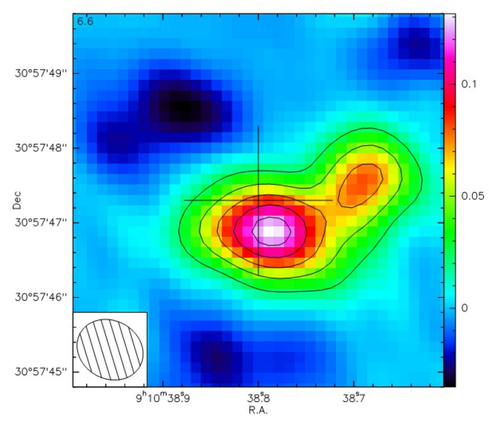

Figure 4: Continuum subtracted CO1−0 channel map at 6.6 kms^{-1}. The contour levels are separated by steps of 24 mJy/beam (≡2σ)

CO model

In order to constrain the spatio-kinematic structure of RS Cnc, we have constructed a new model of CO emission taking into account the velocity-dependent emission and absorption of each element along the line of sight. This allows the evaluation of the detected flux from a source of arbitrary geometry. The density, the excitation temperature, and the velocity are defined at each point of the circumstellar shell. The code can then produce synthetic spectral maps that can be compared to the observed ones.

The populations of the rotational levels of the CO molecules are calculated assuming local thermodynamic equilibrium. The temperature is scaled down by a factor ~2, from the form (~r$^{-0.7}$) obtained by Schöier & Olofsson (2001) for its radial dependence using a radiative transfer model of spherical expanding shells. The same temperatures are used to calculate the thermal Doppler broadening, assuming a Maxwellian velocity distribution. We use a stellar CO/H abundance of 4.0×10^{-4} (all carbon in CO, Smith & Lambert 1986) and a radial dependence of the CO abundance as predicted by the photo-dissociation model of Mamon et al. (1988) for a mass loss rate of 1.0×10^{-7} $M_o yr^{-1}$.

The parameters which define the orientation of the polar axis, the radial distribution of velocities, the mass loss rate and their dependence on latitude are adjusted to best fit the velocity spectra in the 7x7 central maps (9.8"x9.8") (**Fig. 6**). The corresponding velocity, flux of matter and density distributions are shown in **Fig. 5.** The best fit is obtained for AI=52°, PA=10° and a total mass loss rate of 1.24×10^{-7} $M_o yr^{-1}$. The velocity is found to increase outward and is typically three to four times larger at the poles than at the equator.

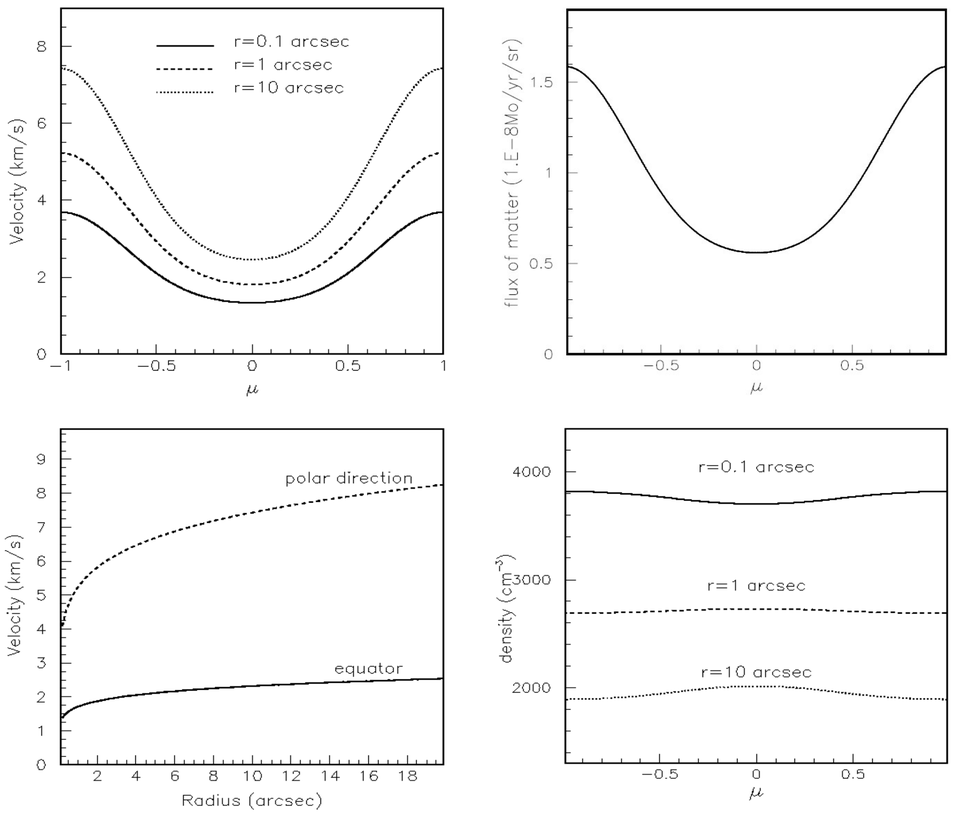

Figure 5: The best fit: sine of latitude (μ) dependence of velocity (up-left), flux of matter (up-right), density (down-right) and r-dependence of the equatorial and polar velocities (down-left).

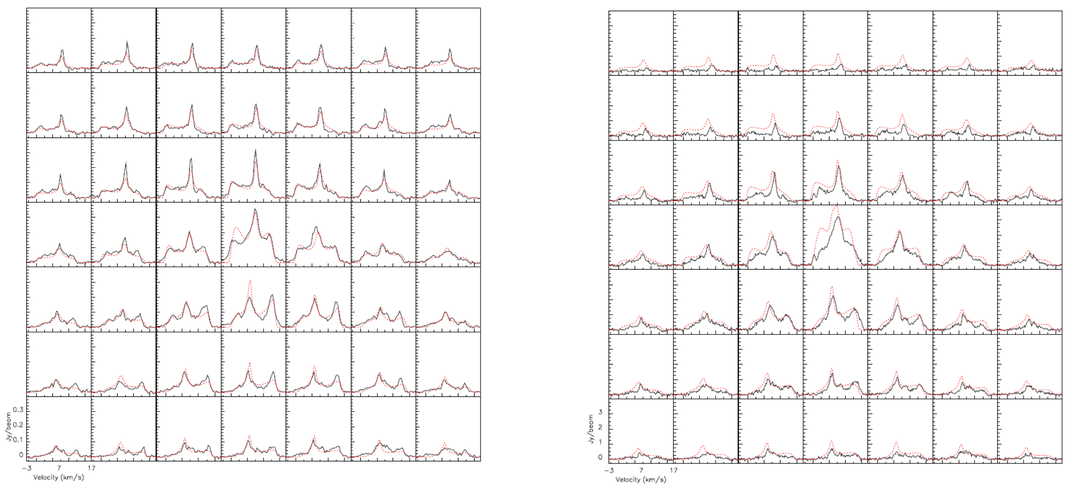

Figure 6: Spectral maps of RS Cnc obtained in CO(1-0) (left) and CO(2-1) (right) with a restoring beam of 1.2". The steps are 1.4" in RA and Dec. The data are in black, and the results of the fit in red.

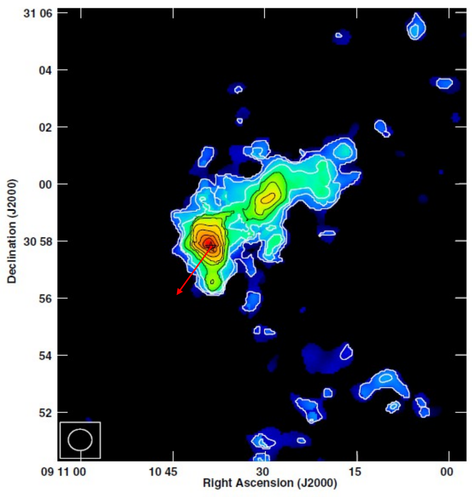

Figure 7: HI total intensity map. Contour levels are (1,2,3...9) × 6.6 Jy beam^{-1}ms^{-1}. This image was derived by summing the emission over the velocity range from 2.6 kms^{-1} to 11.6 kms^{-1}

HI observations

An HI total intensity map based on a combination of VLA C and D configuration data is presented in **Fig. 7**. The HI traces circumstellar gas beyond the molecular dissociation radius and shows a head-tail morphology. The head is elongated in a direction consistent with the polar axis observed in CO. The tail trails the direction of space motion of the star (indicated by an arrow). The measured HI mass is ~0.0055 M_{sun}.The lower limit of timescale for the formation of the tail ∼64 × 10^3 years.

References: *Adelman, S. J., & Dennis, J. W. 2005, Baltic Astron., 14, 41; Dumm, T., & Schild, H. 1998, New Astron., 3, 137; Hoai D.T. et al., 2014, A&A 565, A54; Libert, Y. et al., 2010, A&A, 515, A112; Mamon, G. A. et al., 1988, ApJ, 328, 797; Schöier, F. L., & Olofsson, H. 2001, A&A, 368, 969; Smith, V. V., & Lambert, D. L. 1986, ApJ, 311, 843.*

Acknowledgements: We thank the LIA FVPPL, the PCMI, and the ASA (CNRS) for financial support. LDM gratefully acknowledges financial support from the National Science Foundation through award AST-1310930. Financial and/or material support from the Institute for Nuclear Science and Technology, Vietnam National Foundation for Science and Technology Development (NAFOSTED) under grant number 103.08-2012.34 and World Laboratory is gratefully acknowledged.